Brief Papers

Distributed Supervisory Predictive Control of Distributed Wind and Solar Energy Systems

Wei Qi, Jinfeng Liu, and Panagiotis D. Christofides, *Fellow, IEEE*

***Abstract*—In this work, we design a distributed supervisory model predictive control (MPC) system for optimal management and operation of distributed wind and solar energy generation systems integrated into the electrical grid to facilitate the development of the so-called "smart electrical grid". We consider a topology in which two spatially distributed energy generation systems, a wind subsystem and a solar subsystem, are integrated in a DC power grid, providing electrical power to a local area, and each subsystem is coupled with an energy storage device. A supervisory MPC optimization problem is first formulated to take into account optimality considerations on system operation and battery maintenance; then a sequential and an iterative distributed supervisory MPC architectures are developed to coordinate the actions of the subsystems accordingly. Simulations of 24-hour system operation are carried out under the different control architectures to demonstrate the applicability and effectiveness of the distributed supervisory predictive control design.**

***Index Terms*—Distributed control, distributed energy generation, electrical grid, solar energy systems, supervisory model predictive control, wind energy systems.**

I. Introduction

In a traditional electrical grid, electrical power generated by large, centralized power plants is transmitted to end users using one-directional power flows. In recent years there have been many calls for the development of the so-called "smart electrical grid" (e.g., [1]–[3]) by expanding the traditional electrical grid with distributed, medium-scale renewables-based energy generation systems to better meet the increasing energy demand and environmental regulations. A "smart electrical grid" is expected to be more reliable, more energy efficient and more environmentally friendly. Specifically, it is possible to integrate distributed energy resources and generation systems, like wind and solar systems, into the electrical grid.

Manuscript received September 13, 2011; revised December 02, 2011; accepted December 12, 2011. Manuscript received in final form December 15, 2011. Date of publication January 11, 2012; date of current version February 14, 2013. Recommended by Associate Editor S. Varigonda.

W. Qi and J. Liu are with the Department of Chemical and Biomolecular Engineering, University of California, Los Angeles, CA 90095-1592 USA (e-mail: qiwei.0216@gmail.com; jinfeng@ucla.edu).

P. D. Christofides is with the Department of Chemical and Biomolecular Engineering, University of California, Los Angeles, CA 90095-1592 USA, and also with the Department of Electrical Engineering, University of California, Los Angeles, CA 90095-1592 USA (e-mail: pdc@seas.ucla.edu).

Color versions of one or more of the figures in this paper are available online at http://ieeexplore.ieee.org.

Digital Object Identifier 10.1109/TCST.2011.2180907

Most of the results on the control of wind and solar systems have focused on isolated wind or solar systems. Specifically, there is a significant body of literature dealing with control of wind-based energy generation systems (see, for example, [4], [6], [7] for results and references in this area), while several contributions have been made to the control of solar-based energy generation systems (see, for example, [8]–[10]). There are also a few pieces of work on the regulation of stand-alone [13], [14] and grid-connected [15] hybrid wind-solar energy generation systems. However, little attention has been given to the development of supervisory control systems for hybrid wind-solar energy generation systems that take into account system maintenance and optimal system operation considerations, except from some recent efforts [16], [17]. In [16], a supervisory MPC method was proposed for short-term optimal management and operation of hybrid wind-solar energy generation systems in which the supervisory control system was designed via MPC. In [17], a computationally efficient supervisory control system was designed for long-term optimal management and operation of an integrated wind-solar energy generation and a reverse-osmosis (RO) water desalination system. However, the centralized nature of the supervisory MPC architecture which was used in [16] and [17], may impede its potential for large-scale implementation. For example, the evaluation time of a centralized supervisory MPC may increase significantly with the increase of optimization variables and may exceed the limit for real-time implementation, as well as failures of one or several sensors and actuators may result in consequences such as collapse of the entire centralized control system. These considerations motivated us to develop [18] a conceptual distributed control framework for integrating distributed renewable energy generation systems with the electrical grid, controllable loads and storage systems but did not carry out a detailed control system design or a closed-loop implementation. On the other hand, there have been extensive recent studies with respect to the development of distributed MPC architectures (see, for example, [19]–[24]) but their potential applicability to control of distributed energy systems has not been studied.

In the present work, a distributed supervisory MPC system is designed for the optimal management and operation of distributed wind and solar energy generation systems integrated into the electrical grid. We consider a topology in which a wind subsystem and a solar subsystem are integrated in a direct current (DC) power grid in a distributed fashion, providing electrical power to a local area, and each subsystem is coupled with an energy storage device. We first formulate a supervisory MPC

problem that takes into account optimality considerations on system operation and battery maintenance; then a sequential and an iterative distributed supervisory MPC architectures are developed to coordinate the actions of the subsystems. Simulations of 24-hour system operation are carried out to demonstrate the applicability and effectiveness of the distributed supervisory predictive control designs.

II. Distributed Energy Generation Systems

In a subset of a typical "smart-grid" topology, a wind subsystem and a solar subsystem are integrated into a DC power grid in a distributed fashion, providing electrical power to a local area in which a number of end-users are involved. Each subsystem is also coupled with an energy storage device (lead-acid battery bank) to be used to store excessive energy and to prevent an energy supply shortage. Note that this topology can be expanded to incorporate a large number of diversified energy generation systems which can be geographically isolated to each other. Specifically, the wind system consists of a fixed pitch wind turbine, a multipolar permanent-magnet synchronous generator (PMSG), a rectifier, a DC/DC converter and an auxiliary battery bank denoted as Battery Bank 1. Please refer to [11] for detailed modeling of the wind subsystem. The dynamics of the wind energy generation subsystem can be represented by three state equations describing the time derivatives of the quadrature current i_q, the direct current i_d, in a rotor reference frame and the electrical angular speed ω_e. A sliding mode control technique proposed in [5] is adopted to control the operating point of the wind turbine by manipulating the duty cycle of the converter which commands the voltage across the PMSG terminals. The power generated by the wind subsystem can be expressed as $P_w = i_w v_{b_1}$, where $i_w = (\pi)/(2\sqrt{3})\sqrt{i_q^2 + i_d^2}u_w$ denotes the output current of the wind subsystem, v_{b_1} is the voltage across the terminals of Battery Bank 1 and u_w is the control signal (duty cycle of the DC/DC converter). The solar subsystem involves a photovoltaic (PV) panel array, a DC/DC converter and a battery bank denoted as Battery Bank 2. Two state variables, the voltage across the PV array terminals, $v_{\rm pv}$, and the output current i_s, are used to characterize its dynamics. For the detailed mathematical model and control of the solar subsystem, please refer to [12]. The power delivered by the solar subsystem can be computed as $P_s = i_s v_{b_2}$ where v_{b_2} is the solar subsystem output voltage.

Battery Banks 1 and 2 can be both modeled as a voltage source E_b connected in series with a resistance $R_{b,i}$ and a capacitance $C_{b,i}$ $(i = 1, 2)$. As the voltage drop on $R_{b,i}$ and $C_{b,i}$ is very small compared with E_b, for simplicity, we assume a constant battery voltage, i.e., $v_{b_1} = v_{b_2} = E_b$ which is the imposed voltage of the DC power grid. Moreover, the state of charge (SOC) $s_{b,i}$ and the depth of discharge $d_{b,i}$ of the battery banks are calculated as $s_{b,i}(t) = 1 - d_{b,i}(t) = (Q_{c,i})/(Q_{c,i}^{\max}) = (\int_0^t i_{b,i}(\tau)d\tau)/(Q_{c,i}^{\max})$, where $Q_{c,i}^{\max}$ $(i = 1, 2)$ is the maximum capacity of the Battery Bank i and $i_{b,i}$ is the current across Battery Bank i. Note that the inputs/outputs of the battery banks are the charge/discharge currents which affect the states of charge of the batteries. $Q_{c,i}$ is the current energy storage of the Battery i in ampere hour. The distributed energy systems are coordinated to deliver electrical power to the DC grid to meet the total power demand P_d given by the load current i_L (i.e., $P_d = i_L E_b$) while the batteries are being charged/discharged during the system operation. Assuming ideal voltage inverters, an energy balance equation can be obtained in the form of currents as follows $i_w + i_s = i_{b_1} + i_{b_2} + i_L$.

III. Control Problem Formulation and Design

In this work, we design distributed supervisory control systems for spatially distributed wind and solar energy generation systems. The objective of the distributed supervisory control system is to determine the optimal reference trajectories of the hourly wind and solar power generation $(P_w^{\rm ref}, P_s^{\rm ref})$ and the charge/discharge currents of the two battery banks $(i_{b_1}^{\rm ref}, i_{b_2}^{\rm ref})$ while accounting for a series of optimization considerations and constraints. Specifically, the primary goal of the supervisory control system is to operate the wind and solar systems as well as the battery banks to generate enough energy to meet the power demand of a given local area. In order to achieve this goal, we utilize future weather forecast information and predictions of future power demand of the loads. The reader may refer to [25] for extensive work in short-term forecasting for weather conditions and power consumption. We explicitly account for the following considerations on the battery banks maintenance according to [26] and [27] as follows.

1) Small charge/discharge currents are favorable, as large charge/discharge currents result in more energy dissipated in the battery internal resistance.
2) The charge current should be constrained under a certain upper bound which is a monotonically increasing function of the depth of discharge (DOD) of the battery banks. In this work, we set the upper bounds of the charge currents based on a taper charging approach [26].
3) The DOD of Battery Bank i should not exceed the upper bound $d_{b,i}^{\max}$ in order to protect the battery bank.
4) The batteries should be charged if extra generated power is available (in addition to satisfying power demand).

Specifically, we propose the following cost function to be minimized in the supervisory MPC optimization problem:

$$\begin{aligned} J(t_k) = \alpha \int_{t_k}^{t_{k+N}} & \left| P_d^{\rm for}(t\,|\,t_k) - P_w^{\rm ref}(t\,|\,t_k) - P_s^{\rm ref}(t\,|\,t_k) \right. \\ & \left. + i_{b_1}^{\rm ref}(t\,|\,t_k)E_b + i_{b_2}^{\rm ref}(t\,|\,t_k)E_b \right| dt \\ & + \beta_1 \int_{t_k}^{t_{k+N}} i_{b_1}^{\rm ref}(t\,|\,t_k)^2\, dt \\ & + \beta_2 \int_{t_k}^{t_{k+N}} i_{b_2}^{\rm ref}(t\,|\,t_k)^2\, dt + \gamma_1 \int_{t_k}^{t_{k+N}} d_{b_1}(t)^2\, dt \\ & + \gamma_2 \int_{t_k}^{t_{k+N}} d_{b_2}(t)^2\, dt + \delta \int_{t_k}^{t_{k+N}} P_s^{\rm ref}(t\,|\,t_k)\, dt \quad (1) \end{aligned}$$

where N is the prediction horizon of the MPC, $P_d^{\rm for}(t\,|\,t_k)$ is the forecast power demand at time t $(t \in [t_k, t_{k+N}))$ predicted at time t_k and α, β_1, β_2, γ_1, γ_2, and δ are positive weight factors. The first term in the cost function penalizes the gap between the scheduled wind/solar/battery power delivery to the

electrical grid and the forecast power demand from the local consumers, thus driving the two distributed systems to satisfy the power demand to the maximum extent. The second and the third terms prevent the charge/discharge currents of the Battery 1 and 2 from surging, respectively, so as to maintain an acceptable internal cell temperature and prevent electrolyte dry-out. Besides, large charge/discharge current flowing through the internal cell resistance dissipates more energy. The fourth and the fifth terms drive the two batteries to be fully charged when surplus energy is available by penalizing their depths of discharge so that they can make full use of the battery capacities to counter a possible power shortage in the future. The last term in the cost function implies that the wind energy generation system is operated as the primary generation system while the solar energy generation system is activated when necessary. Note that in sizing the capacities of the batteries, larger variations in environmental conditions require more capacity investment of the batteries so as to reduce the possibility of unexpected power shortage brought about by unfavorable weather or sudden demand surge. However, there are also other factors that affect the sizing of the batteries. Primarily, the battery storage capacity should be comparable to the capacity of its affiliated generator; and it may also be favorable to have additional capacity space for power trading, that is, to store more energy than needed by generating or by purchasing from the grid when electricity price is low and sell it to the grid when the price is high. Also note that the weight factors in the cost function are carefully tuned to account for the following priority considerations: 1) the power demand should be satisfied under any conditions; 2) when 1) is ensured, the terms concerning the state of charge of the batteries become dominant, followed by the terms on charge/discharge current; and 3) a slight weight is assigned to the last term only to ensure that the MPC optimization problem has a unique solution at any time.

A. Centralized Supervisory MPC Architecture

We first present a centralized supervisory MPC architecture where the MPC problem at time t_k is formulated as

$$\min_{T_l^{\mathrm{ref}}(t\,|\,t_k)\in S(\Delta)} J(t_k) \tag{2a}$$

$$\text{s.t. } 0 \le P_w^{\mathrm{ref}}(t\,|\,t_k) \le \min_t \left\{P_w^{\max}(t\,|\,t_k)\right\}, \quad t \in [t_{k+j}, t_{k+j+1}) \tag{2b}$$

$$0 \le P_s^{\mathrm{ref}}(t\,|\,t_k) \le \min_t \left\{P_s^{\max}(t\,|\,t_k)\right\}, \quad t \in [t_{k+j}, t_{k+j+1}) \tag{2c}$$

$$0 \le d_{b,i}(t) \le d_{b,i}^{\max}, i = 1, 2 \tag{2d}$$

$$i_{b,i}^{\mathrm{ref}}(t\,|\,t_k) \le i_{b,i}^{\max}(s_{b,i}(t)), i = 1, 2 \tag{2e}$$

$$\dot{\tilde{x}}(t) = f(\tilde{x}(t)) + g(\tilde{x}(t))u(t) \tag{2f}$$

$$h(\tilde{x}) = 0,\ \tilde{x}(t_k) = x(t_k). \tag{2g}$$

In the above optimization problem, $T_l^{\mathrm{ref}}(t\,|\,t_k), l = 1, 2, 3, 4$, denote reference trajectories $P_w^{\mathrm{ref}}(t\,|\,t_k)$, $i_{b_1}^{\mathrm{ref}}(t\,|\,t_k)$, $P_s^{\mathrm{ref}}(t\,|\,t_k)$ and $i_{b_2}^{\mathrm{ref}}(t\,|\,t_k)$, respectively. Δ is the sampling time and $S(\Delta)$ denotes the family of piece-wise constant functions and $j = 0, \ldots, N-1$, indicating that the control actions of the MPC are constant within each sampling time. Equations (2b)–(2e) impose constraints on the trajectories of the decision variables as well as on the depths of discharge of the Battery Banks 1 and 2. Specifically, $P_w^{\max}(t\,|\,t_k)$ and $P_s^{\max}(t\,|\,t_k)$ are the maximum available powers predicted at time t_k that can be generated by the wind and the solar subsystems at time t, respectively, estimated based on the information of the weather forecast [16]. $d_{b,i}^{\max}$ is the upper bound on the depth of discharge of the Battery Bank i and $i_{b,i}^{\max}(s_{b,i}(t))$ is the upper bound on the charge current of the Battery Bank i, which is a function of the state of charge, following the taper charging strategy. In addition, in (2f)–(2g), $\tilde{x}$ and u are the predicted future state and control input trajectories of the distributed system, respectively, and f and g are nonlinear vector functions representing the state space and $h(\cdot)$ is the local control law which guarantees that the system tracks the power reference values [16], [13]. We consider all turbine and solar dynamics as fast and at quasi-steady state in the model used in all the MPCs; however, in the model used to simulate the closed-loop system and where we implement both the distributed supervisory MPC and the local control scheme, the full-order plant model is used accounting explicitly for the dynamics of all subsystems. Specifically, we note that the dynamics of the state variables in the wind/solar energy generation subsystems have transient time in the time scale of a few seconds. Therefore, when solving a long-term (e.g., one-day) MPC problem, the steady state assumption can be safely made in the model used in the supervisory MPC. In this way, we exploit the "two-time-scale" behavior of the system and significantly increase the efficiency of the MPC problem evaluation without much loss of accuracy (see also [17]). At each sampling time t_k, the supervisory MPC problem of (2) is updated and solved, providing the optimal trajectories denoted as $T_l^{\mathrm{ref},*}(t\,|\,t_k), l = 1, 2, 3, 4$. Subsequently, the supervisory controller sends the reference values to the local controllers.

B. Distributed Supervisory MPC Architecture

We utilize two distributed MPC (DMPC) architectures, sequential and iterative, for large scale nonlinear systems developed in [23]; please see [21] and [22] for further important results on distributed design. A schematic of the distributed supervisory MPC system is shown in Fig. 1. The centralized supervisory MPC controller is replaced with two distributed supervisory MPC controllers, each of which is responsible for providing optimal reference trajectories to the local controller of each corresponding subsystem. Accordingly, the supervisory MPC problem of (2) is decoupled into two distributed MPC problems with the global cost function (2a). Specifically, the supervisory MPC 1 problem can be expressed as follows:

$$\min_{P_w^{\mathrm{ref}}(t\,|\,t_k), i_{b_1}^{\mathrm{ref}}(t\,|\,t_k)\in S(\Delta)} J(t_k) \tag{3a}$$

$$\text{s.t. } 0 \le P_w^{\mathrm{ref}}(t\,|\,t_k) \le \min_t \left\{P_w^{\max}(t\,|\,t_k)\right\}, \quad t \in [t_{k+j}, t_{k+j+1}) \tag{3b}$$

$$0 \le d_{b_1}(t) \le d_{b_1}^{\max} \tag{3c}$$

$$i_{b_1}^{\mathrm{ref}}(t\,|\,t_k) \le i_{b_1}^{\max}(s_{b_1}(t)) \tag{3d}$$

$$\dot{\tilde{x}}(t) = f(\tilde{x}(t)) + g(\tilde{x}(t))u(t) \tag{3e}$$

$$h(\tilde{x}) = 0,\ \tilde{x}(t_k) = x(t_k) \tag{3f}$$

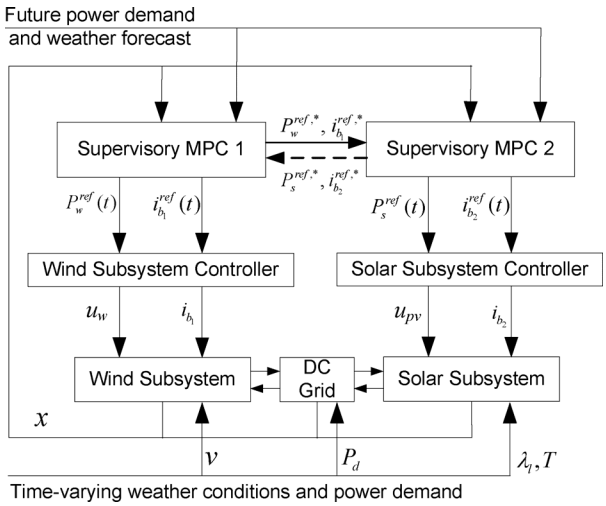

Fig. 1. Distributed supervisory MPC control system. v, P_d, λ_t and T are wind speed, power demand, insolation and cell temperature, respectively.

and as follows for the supervisory MPC 2:

$$\min_{P_s^{\mathrm{ref}}(t\,|\,t_k),i_{b_2}^{\mathrm{ref}}(t\,|\,t_k)\in S(\Delta)} J(t_k) \tag{4a}$$

$$\text{s.t. } 0 \le P_s^{\mathrm{ref}}(t\,|\,t_k) \le \min_t \{P_s^{\max}(t\,|\,t_k)\}, \quad t \in [t_{k+j}, t_{k+j+1}) \tag{4b}$$

$$0 \le d_{b_2}(t) \le d_{b_2}^{\max} \tag{4c}$$

$$i_{b_2}^{\mathrm{ref}}(t\,|\,t_k) \le i_{b_2}^{\max}(s_{b_2}(t)) \tag{4d}$$

$$\dot{\tilde{x}}(t) = f(\tilde{x}(t)) + g(\tilde{x}(t))u(t) \tag{4e}$$

$$h(\tilde{x}) = 0,\ \tilde{x}(t_k) = x(t_k). \tag{4f}$$

Note that the dimensions of optimization variables with respect to the above two optimization problems are reduced to be $m_w N$ and $m_s N$, respectively, where $m_w = m_s = 2$ are the numbers of trajectories to be optimized in the wind and the solar subsystems, respectively. Again, all state measurements of the wind/solar subsystems, their slow-dynamics models and the forecast of the future power demand and weather forecast are available to both supervisory controllers at each sampling time and they are interconnected by a communication network. Additionally, we assume that the optimal solutions of the optimization problems of (3) and (4) obtained in the previous sampling interval, $P_w^{\mathrm{ref},p}(t\,|\,t_{k-1})$, $i_{b_1}^{\mathrm{ref},p}(t\,|\,t_{k-1})$, $P_s^{\mathrm{ref},p}(t\,|\,t_{k-1})$, and $i_{b_2}^{\mathrm{ref},p}(t\,|\,t_{k-1})$, or denoted as $T_l^{\mathrm{ref},p}(t\,|\,t_{k-1}), l = 1, 2, 3, 4$, for simplicity, are available at the current sampling time; and the initial trajectory guesses for the current optimization problems is taken as their latest $N-1$ elements plus one step zero-order extrapolation, which can be expressed as follows:

$$T_l^{\mathrm{ref},0}(t\,|\,t_k) = \begin{cases} T_l^{\mathrm{ref},p}(t\,|\,t_{k-1}) & t \in [t_k, t_{k+N-1}) \\ T_l^{\mathrm{ref},p}(t-\Delta\,|\,t_{k-1}) & t \in [t_{k+N-1}, t_{k+N}). \end{cases} \tag{5}$$

In what follows, we develop two distributed supervisory MPC architectures which coordinate the two supervisory MPC controllers in different fashions.

1) Sequential Distributed Supervisory MPC: Under the architecture of sequential distributed supervisory MPC, the communication channel shown in Fig. 1 is one-directional from the supervisory MPC 1 to the supervisory MPC 2. The implementation strategy is as follows:

1) At each t_k, the supervisory MPC 1 and 2 receive the state measurements $x(t_k)$ from the sensors and update the forecast of weather conditions and power demand.
2) Supervisory MPC 1
   a) The supervisory MPC problem of (3) is evaluated based on $x(t_k)$ and the initial trajectories guess $T_l^{\mathrm{ref},0}$ set according to (5).
   b) The supervisory MPC 1 sends the first steps of the optimal reference trajectories $P_w^{\mathrm{ref},*}$ and $i_{b_1}^{\mathrm{ref},*}$ to the wind subsystem local controller for implementation and the entire optimal trajectories to the supervisory MPC 2.
3) Supervisory MPC 2
   a) The supervisory MPC problem of (4) is evaluated based on $x(t_k)$ and the initial trajectories guess set as $P_w^{\mathrm{ref},*}$, $i_{b_1}^{\mathrm{ref},*}$, $P_s^{\mathrm{ref},0}$ and $i_{b_2}^{\mathrm{ref},0}$.
   b) The supervisory MPC 2 sends the first steps of the optimal reference trajectories $P_s^{\mathrm{ref},*}$ and $i_{b_2}^{\mathrm{ref},*}$ to the solar subsystem local controller for implementation.

Note that in this case the supervisory MPC problems of (3) and (4) are evaluated in sequence and once at each sampling time. Therefore, the reference trajectories $P_w^{\mathrm{ref},*}$ and $i_{b_1}^{\mathrm{ref},*}$ are optimal only with respect to $P_s^{\mathrm{ref},0}$ and $i_{b_2}^{\mathrm{ref},0}$, which may result in suboptimality of the whole system. Note that we follow the "wind-solar" sequence because we assume that the wind subsystem has larger capacity than the solar subsystem and reason that this sequence, generally, provides a solution closer to the optimum corresponding to the centralized supervisory MPC compared with the reverse sequence.

2) Iterative Distributed Supervisory MPC: An alternative to the architecture of the sequential distributed supervisory MPC is to evaluate the supervisory MPC problems of (3) and (4) in parallel and iterate to improve the closed-loop performance. In this architecture, a bi-directional communication channel is utilized to interconnect the two distributed supervisory controllers. When a new state measurement is available at a sampling time, both distributed supervisory MPC controllers evaluate and then broadcast their future reference trajectories to each other. On the basis of the newly received as well as previously retained reference trajectories, this process of parallel evaluation and broadcast is carried out again and repeated until the maximum iteration number $c_{\max}$ is reached. Upon the termination of iterations, the reference trajectories of the iteration step which provides the minimum value of the cost function of (1) are chosen for implementation by the local controllers. The specific implementation strategy of the iterative distributed supervisory MPC is stated as follows:

1) At each t_k, the supervisory MPC controllers 1 and 2 receive the state measurements $x(t_k)$ from the sensors and update the forecast of weather conditions and power demand. The initial trajectory guesses $T_l^{\mathrm{ref},0}$ are set according to (5) for the supervisory MPC problem of (3) and (4).

2) At iteration c $(1 \leq c \leq c_{\max})$
   a) The supervisory MPC problems (3) and (4) are solved in parallel based on $x(t_k)$ and the initial trajectory guesses.
   b) The supervisory MPC controllers 1 and 2 exchange their newly obtained future reference trajectories $P_w^{\mathrm{ref},n}(t\,|\,t_k)$, $i_{b_1}^{\mathrm{ref},n}(t\,|\,t_k)$, $P_s^{\mathrm{ref},n}(t\,|\,t_k)$ and $i_{b_2}^{\mathrm{ref},n}(t\,|\,t_k)$, or for simplicity denoted as $T_l^{\mathrm{ref},n}(t\,|\,t_k), l = 1,2,3,4$ (n indicates "newly obtained"), through bi-direction communication.
   c) The reference trajectories obtained at iteration c are calculated as follows:

$$T_l^{\mathrm{ref},c}(t\,|\,t_k) = (1-\eta)T_l^{\mathrm{ref},c-1}(t\,|\,t_k) + \eta T_l^{\mathrm{ref},n}(t\,|\,t_k) \quad (6)$$

   where $\eta \in (0,1]$ is a tuning parameter controlling the rate of updating the reference trajectories at each iteration. The reference trajectories at iteration c as well as the the corresponding value of the cost function defined by (1) are then stored in both supervisory controllers. When $c < c_{\max}$, (6) is also used to compute the initial trajectory guesses for iteration $c+1$.
3) Upon completion of $c_{\max}$ iterations, the optimal reference trajectories are determined by the reference trajectories of the iteration c that provides the minimum value of the cost function, as follows:

$$T_l^{\mathrm{ref},*}(t\,|\,t_k) = \arg \min_{T_l^{\mathrm{ref},c}(t\,|\,t_k) \in S(\Delta)} J(t_k) \quad (7)$$

   with $c = 1, \ldots, c_{\max}$. The supervisory MPC controllers 1 and 2 then send their first step of the optimal reference trajectories to the wind/solar subsystems local controllers, respectively.

Note that under this architecture, the parameters η and $c_{\max}$ are tuning parameters for the iterative distributed MPC. η controls the rate of updating the reference trajectories at each iteration (i.e., how fast the new reference trajectories can deviate from the previous ones) and $c_{\max}$ is the maximum iteration number which implicitly determines the time that will be used in the optimization calculation at each sampling time. In general, these parameters can be picked based on experiments. In our simulations, the values for the two parameters were determined via extensive simulations. Specifically, an over-conservative choice (i.e., η being close to zero) requires too many iterations before satisfactory reference trajectories can be obtained in the sense of the entire system performance, while being too aggressive (i.e., η being close to one) may result in non-convergence of the solutions given by the two distributed supervisory MPCs. Similarly, a balance should also be struck between the overall evaluation time and the system performance in choosing the maximum iteration $c_{\max}$. Furthermore, one can expect that the implementation of these designs is able to reduce the computational burden in the evaluation of the optimization problem with less optimization variables in each supervisory MPC controller. However, this reduction in the evaluation may lead to increased communication; and in order to achieve (if possible) the optimal solution given by a centralized MPC, the increased number of iterations of the iterative MPC may result in more computational time. However, we noted that the reduction of evaluation time in each distributed MPC evaluations makes the use of smaller sampling time in MPC possible at the expense of performance cost. Besides, there is no guarantee that the solution of the optimization problem of (2) provided by the distributed supervisory MPC can converge to that by the centralized supervisory MPC, which is illustrated in the last subsection of the simulation results.

C. Design of Local Controllers

The objective of the wind subsystem controller is to drive the wind energy generation subsystem to track the operating reference value $P_w^{\mathrm{ref}}(t)$ sent from the supervisory control system. Similar to our previous work [17], we follow the nonlinear controller design proposed in [5] to design the local controller for the wind subsystem. For the solar subsystem controller, the local controller drives the solar energy generation subsystem to track the reference value $P_s^{\mathrm{ref}}(t)$. We also follow the nonlinear controller design proposed in [12] to design this local controller. In each energy generation subsystem, two operation modes are used: when the real weather conditions permit the power generation as the reference value dictates, the reference is tracked; otherwise, a maximum power point tracking approach is implemented. As to the regulation of the Battery Banks 1 and 2, the real-time charge/discharge currents are determined by the current balance and adopt the following control strategy for $i = 1, 2$ (see also [26]):

$$i_{b,i}(t) = i_{b,i}^{\mathrm{ref}}(t) + \frac{Q_{c,i}^{\max}}{Q_{c,1}^{\max} + Q_{c,2}^{\max}}(i_w(t) + i_s(t) - i_L(t)). \quad (8)$$

IV. Simulation Results

We carry out simulations of the wind and solar system operation with the sequential, the iterative and the centralized MPC, respectively, in order to demonstrate the effectiveness and applicability of the distributed supervisory MPC design. For comparison purposes, the environmental settings for each set of simulations are set to be identical. The prediction horizon and the sampling time of each MPC are chosen to be $N = 24$ and $\Delta = 1$ h, taking into account that the power demand in a local area usually presents periodic fluctuations with a period of 24 h. In addition, all parameters are tuned to reflect the optimization considerations stated in the previous section. For example, η, which controls the rate of updating reference trajectories, is chosen to be 0.5, since simulations showed that when η was chosen to be over 0.7, the performance cost exhibited oscillation with respect to iteration steps and no longer converges to the value given by the centralized MPC. On the other hand, when η was less than 0.3, the convergence rate of the performance cost became unnecessarily slow. In the cost function, all the weight factors were first assigned initial values so that all terms were in a comparable order of magnitude. Then, α is tuned to be 5. An α less than 2.5 would result in severely power generation insufficiency, whereas too much sacrifices of other optimization considerations would occur with α larger than 7.5. Using similar arguments, the other weight factors are chosen to be $\beta_1 = 0.04$, $\beta_2 = 0.02$, $\gamma_1 = 2500$, $\gamma_2 = 1000$, and $\delta = 0.002$. Note that the parameter tuning is a trial-and-error process with respect to

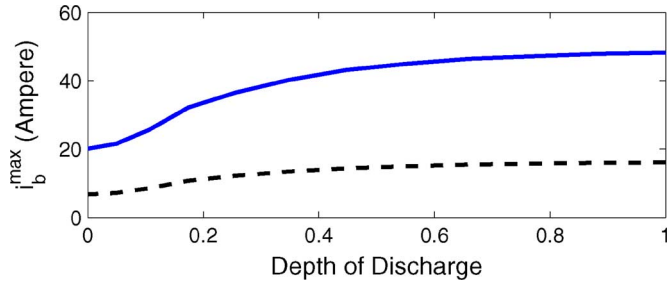

Fig. 2. Upper bounds on charge current of the Battery Bank 1 (solid line) and the Battery Bank 2 (dashed line).

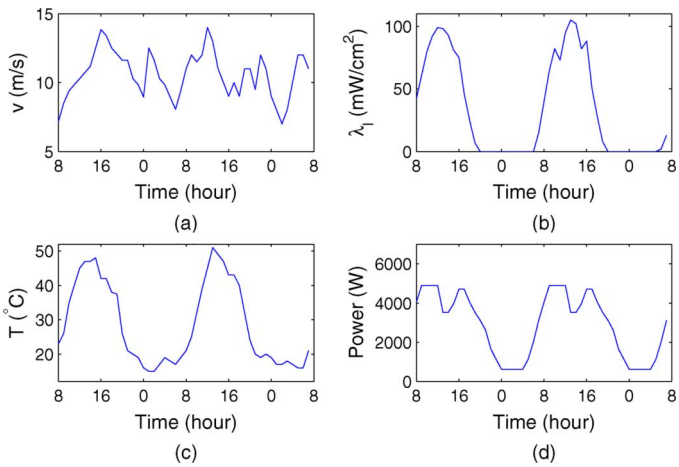

Fig. 3. Forecast of weather conditions and power demand. (a) Wind speed v, (b) insolation λ_l, (c) PV panel temperature T, and (d) power demand P_d.

the specific system scale and topology which we consider in this work. However, the optimization considerations as well as their priorities expressed in Section III can be generalized to the design of other distributed energy generation systems. In all the simulations, the optimization problems of the supervisory MPC are solved by the open source interior point optimizer Ipopt [28] and are under the same optimality options settings. In solving the supervisory MPC problem, the scheduled power generation is constrained within $0 \sim 9000$ W for the wind subsystem and $0 \sim 2500$ W for the solar subsystem. As to the battery coupled to each subsystem, the capacities of the Battery 1 and 2 are chosen to be $Q_{c,1}^{\max} = 420$ Ah and $Q_{c,2}^{\max} = 140$ Ah (ampere-hour), respectively, to be consistent with the wind/solar energy generation system capacities and environment uncertainty. The upper bounds on depth of discharge (DOD) d_{b_1} and d_{b2} are both $d_b^{\max} = 0.8$ and the upper bounds on the battery charge current $i_b^{\max}$ are functions of d_{b1} and d_{b2}, respectively, following a taper charging method as shown in Fig. 2.

A. System Operation

The simulations for 24-h operation are carried out starting at 8 am. We assume that day-ahead weather forecast and power demand requirements are available, noting that hourly weather condition forecast is commercially available and power demand of future 24 h can be estimated based on past energy consumption data. A two-day forecast of wind speed, insolation, PV cell temperature, and power demand is shown in Fig. 3. The uncertainty of environmental variables is a key issue in the design of a wind/solar energy generation system and is taken into account in the distributed supervisory MPC design. The deviations of real hourly wind speed, solar radiance intensity, PV panel temperature and power demand from hour-ahead forecast are mitigated by the coordinated behavior of the energy generation subsystems which are able to update their power generation schedules accordingly; meanwhile, the robustness against high frequency disturbances of these environmental variables is guaranteed by the local controllers implemented on the wind and solar subsystems (see [11]–[13]). In this work, we set up to 15%, 10%, 10%, and 10% hourly deviations in the wind speed, insolation, PV panel temperature and power demand, respectively, and introduce high frequency normally distributed noise to these variables with standard deviations of 7%, 2.5%, 2.5%, and 5%, respectively, which are shown in Fig. 4. Figs. 5–7 show the evolution of wind/solar power generation with the sequential, the iterative ($c_{\max} = 6$) and the centralized supervisory MPC, respectively. In each figure, one can see that the super-

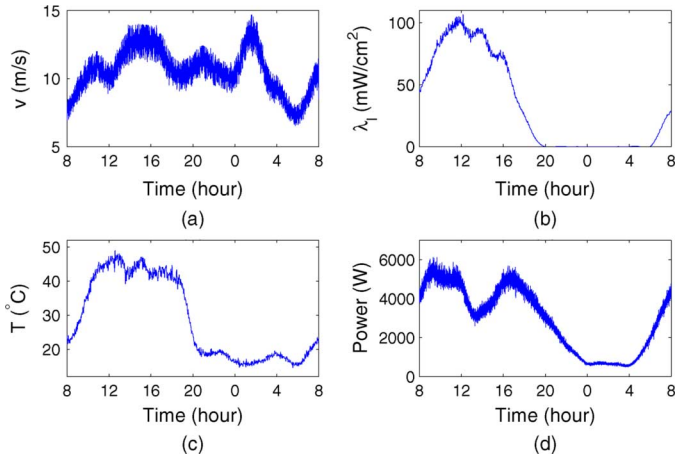

Fig. 4. Weather conditions and power demand. (a) Wind speed v, (b) insolation λ_l, (c) PV panel temperature T, and (d) power demand P_d.

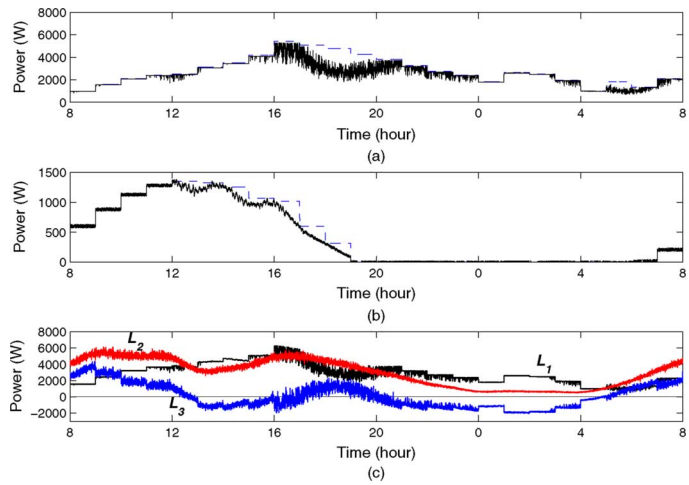

Fig. 5. Power generation and consumption with the sequential supervisory MPC. (a) Power generated by wind subsystem P_w (solid line) and wind power reference P_w^{ref} (dashed line), (b) power generated by solar subsystem P_s (solid line) and solar power reference P_s^{ref} (dashed line), and (c) L_1: generated power $P_w + P_s$, L_2: total power demand P_d, and L_3: the power gap filled by the batteries $P_b = P_d - P_w - P_s$.

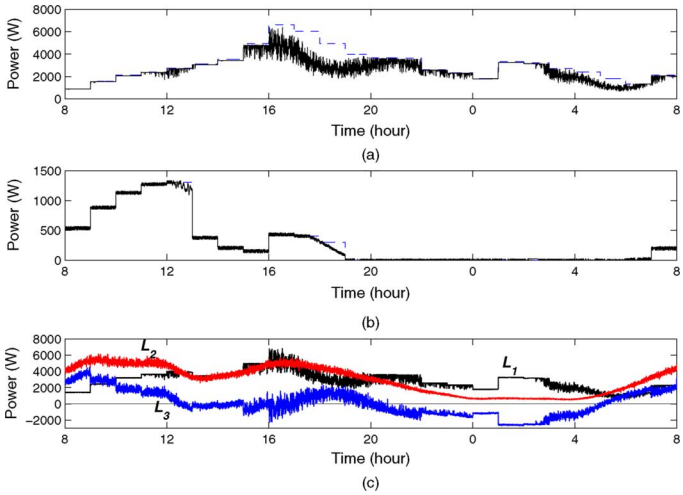

Fig. 6. Power generation and consumption with the iterative supervisory MPC ($c_{\max} = 6$). (a) Power generated by wind subsystem P_w (solid line) and wind power reference P_w^{ref} (dashed line), (b) power generated by solar subsystem P_s (solid line) and solar power reference P_s^{ref} (dashed line), and (c) L_1: generated power $P_w + P_s$, L_2: total power demand P_d, and L_3: the power gap filled by the batteries $P_b = P_d - P_w - P_s$.

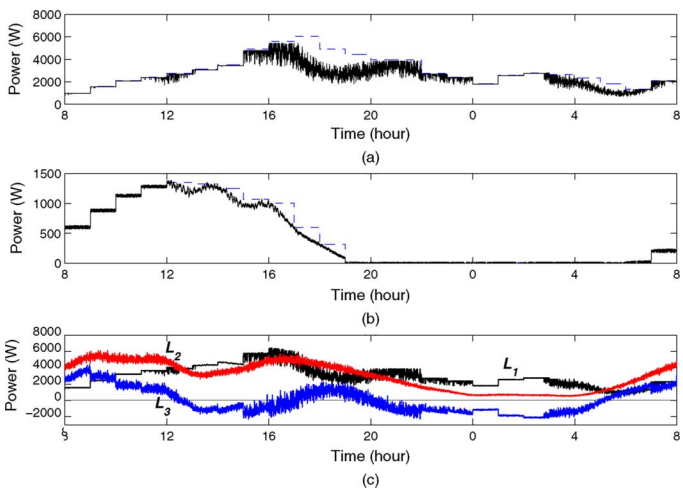

Fig. 7. Power generation and consumption with the centralized supervisory MPC. (a) Power generated by wind subsystem P_w (solid line) and wind power reference P_w^{ref} (dashed line), (b) power generated by solar subsystem P_s (solid line) and solar power reference P_s^{ref} (dashed line), and (c) L_1: generated power $P_w + P_s$, L_2: total power demand P_d, and L_3: the power gap filled by the batteries $P_b = P_d - P_w - P_s$.

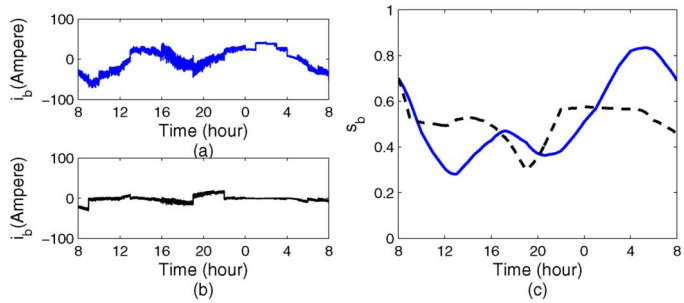

Fig. 8. Time evolution of battery charge/discharge with the sequential supervisory MPC. (a) Charge/discharge current of the Battery 1, (b) charge/discharge current of the Battery 2, and (c) state of charge s_b of the Battery 1 (solid line) and the Battery 2 (dashed line).

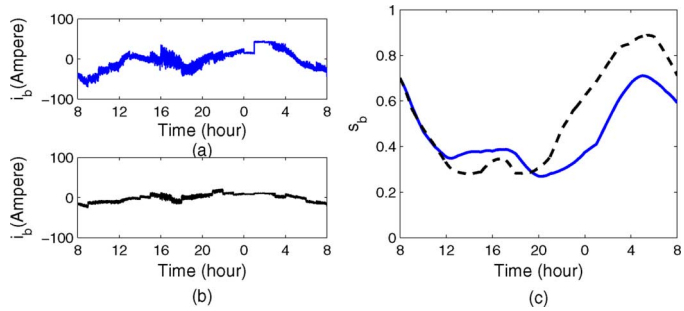

Fig. 9. Time evolution of battery charge/discharge with the iterative supervisory MPC ($c_{\max} = 6$). (a) Charge/discharge current of the Battery 1, (b) charge/discharge current of the Battery 2, and (c) state of charge s_b of the Battery 1 (solid line) and the Battery 2 (dashed line).

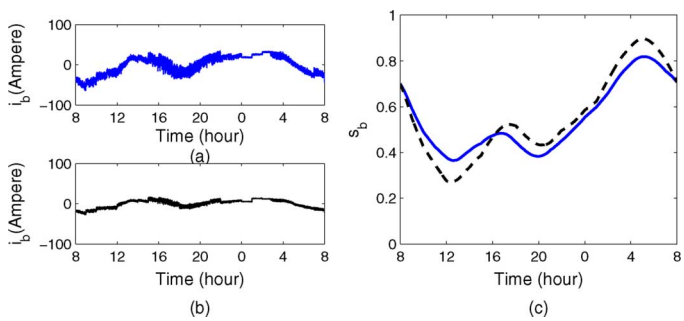

Fig. 10. Time evolution of battery charge/discharge with the centralized supervisory MPC. (a) Charge/discharge current of the Battery 1, (b) charge/discharge current of the Battery 2, and (c) state of charge s_b of the Battery 1 (solid line) and the Battery 2 (dashed line).

visory MPC at the beginning of each hour is able to send optimized wind/solar power generation references for the current hour to the local controllers which drive their respective subsystems accordingly. However, when the reference value is not achievable under the current weather condition during $15 \sim 21$ h and during $3 \sim 7$ h for the wind subsystem, the local controller switches to the operation mode of maximum power point tracking. Moreover, it can be seen from Figs. 5(c), 6(c), and 7(c) that power generation falls into three stages with respect to the supply/demand gap: insufficient ($8 \sim 12$ h and $4 \sim 8$ h), balanced ($12 \sim 20$ h) and excessive ($20 \sim 4$ h). The supervisory MPC coordinates the charge/discharge currents of the two batteries in order to meet the energy gap while making optimized use of their capacities, as shown in Figs. 8–10. Note that the outcome of the battery current is based on $i_{b_1}^{\text{ref}}(t)$ and $i_{b_2}^{\text{ref}}(t)$ at each hour, and the states of charge of the two batteries present periodic charge cycles during the day in each case.

B. *Discussion on Performance of the Distributed MPC*

We next discuss the performance of the distributed supervisory MPC schemes in this application compared with that of the centralized MPC. First, we compare the computational time consumed for solving MPC optimization problems with the different schemes as shown in Table I. Note that in the table the "overall" in the row of sequential MPC can be calculated by $t_1 + t_2$, which means the sum of evaluation times required by the two distributed MPC controllers while in the row of iterative MPC the "overall" equals $\sum_{i=1}^{c_{\max}} \max\{t_{1i}, t_{2i}\}$, denoting

TABLE I
MEAN EVALUATION TIME (s) OF INDIVIDUAL AND OVERALL MPC OPTIMIZATION PROBLEM OF EACH HOUR UNDER DIFFERENT POWER GENERATION CONDITIONS

		Insufficient ($8 \sim 12\ hr$ & $4 \sim 8\ hr$)	Balanced ($12 \sim 20\ hr$)	Excessive ($20 \sim 4\ hr$)	Whole day
Centralized	MPC	43.02	35.62	46.09	41.58
Sequential	MPC1	19.31	5.722	12.06	12.37
	MPC2	2.705	3.929	2.749	3.128
	overall	22.02	9.651	14.81	15.49
Iterative ($c_{max} = 1$)	MPC1	13.18	11.33	0.3753	8.293
	MPC2	7.905	4.299	22.63	11.61
	overall	18.16	11.38	22.65	17.39
Iterative ($c_{max} = 3$)	MPC1	9.597	10.64	4.429	8.221
	MPC2	7.032	2.862	4.354	4.749
	overall	36.89	32.60	22.12	30.54
Iterative ($c_{max} = 6$)	MPC1	7.097	7.385	11.92	8.802
	MPC2	4.453	7.340	6.357	6.050
	overall	47.19	72.59	93.20	71.00
Iterative ($c_{max} = 10$)	MPC1	4.457	5.266	7.055	5.593
	MPC2	3.192	4.081	4.453	3.909
	overall	53.47	70.06	92.26	71.93

the sum of evaluation times of each iteration step which is determined by the maximum of the computational times of the two distributed MPCs. The following observations can be made.

- During each period, the time needed to solve an individual distributed MPC optimization problem, or even the overall time for the sequential MPC, is significantly less than the time needed for the centralized MPC. This is because the number of decision variables involved in the optimization problem is halved in the former case.
- The overall evaluation time for the iterative supervisory MPC increases as the iteration number becomes larger, but not in a linear fashion in general. In fact, one can see that the mean overall evaluation time for the whole day with $c_{\max} = 10$, 71.93 s, is almost equal to the evaluation time (71.00 s) with $c_{\max} = 6$. This results from the fact that the larger number of iterations provides more optimized reference trajectories. The next-hour MPC optimization problem, whose initial guess is based on the last hour solution, can thus be solved in shorter time. This can also be seen from the table that the evaluation time of each individual MPC optimization problem with $c_{\max} = 10$ is less than that with $c_{\max} = 6$. However, it does not necessarily indicate that the performance cost can converge to the cost corresponding to the centralized MPC, which will be further discussed.

We also compare the different control schemes from a performance cost point of view. To be consistent with the cost function in the supervisory MPC optimization problem, the mean performance cost of each hour's system operation is calculated by the following expression:

$$J = \frac{1}{M_t - M_i + 1} \sum_{i=M_i}^{M_t} \Big(\alpha \left| P_d^{\text{for}}(t \,|\, t_i) - P_w^{\text{ref}}(t \,|\, t_i) - P_s^{\text{ref}}(t \,|\, t_i) + i_{b_1}^{\text{ref}}(t \,|\, t_i) E_b + i_{b_2}^{\text{ref}}(t \,|\, t_i) E_b \right| + \beta_1 \bar{i}_{b_1}(i)^2 + \beta_2 \bar{i}_{b_2}(i)^2 + \gamma_1 \bar{d}_{b_1}(i)^2 + \gamma_2 \bar{d}_{b_2}(i)^2 + \delta \bar{P}_s(i) \Big) \tag{9}$$

where M_i and M_t are the initial hour and the terminal hour of the period to be considered and $\bar{i}_{b1}(i), \bar{i}_{b2}(i), \bar{d}_{b1}(i), \bar{d}_{b2}(i)$, and $\bar{P}_s(i)$ are mean values in hour i. Each term after the summation symbol corresponds to a term in the cost function of (1) with the weigh factors unchanged. Note that the high frequency fluctuations are not taken into account in the cost evaluation.

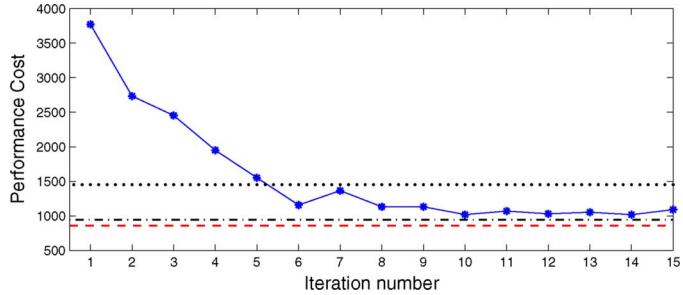

Fig. 11. Mean performance cost J of each hour. (a) Iterative MPC (solid line): For $c_{\max} = 1 \sim 15$, $J = 3771.2, 2734.3, 2453.9, 1951.1, 1552.9, 1156.8, 1365.11131.9, 1132.7, 1019.0, 1069.4, 1030.9, 1054.2, 1018.4, 1090.6,$ respectively, (b) centralized MPC ($J = 857.54$) (dashed line), (c) sequential MPC ($J = 944.12$) (dash-dotted line), and (d) reversed sequential MPC ($J = 1453.0$) (dotted line).

TABLE II
MEAN PERFORMANCE COST OF EACH HOUR UNDER DIFFERENT POWER GENERATION CONDITIONS

	Insufficient ($8 \sim 12\ hr$ & $4 \sim 8\ hr$)	Balanced ($12 \sim 20\ hr$)	Excessive ($20 \sim 4\ hr$)	Whole day
Centralized	581.22	1239.3	752.05	857.54
Sequential	688.24	1263.5	880.59	944.12
Sequential (reversed)	736.31	1974.3	1648.2	1453.0
Iterative ($c_{max} = 1$)	3337.3	3275.5	4700.7	3771.2
Iterative ($c_{max} = 3$)	1487.7	3041.3	2823.6	2450.9
Iterative ($c_{max} = 6$)	664.13	1525.9	1280.3	1156.8
Iterative ($c_{max} = 10$)	621.92	1414.8	1020.2	1019.0

From Table II and Fig. 11, one can see that the centralized MPC provides the lowest performance cost. As the iteration number increases, the performance cost given by the iterative MPC decreases significantly and converges to a value which is slightly larger than the value corresponding to the sequential MPC. However, this does not indicate that the sequential MPC is superior to the iterative MPC in general, as can be seen from the reversed sequential MPC in which case we adopt a solar/wind sequence. Also note that due to the high nonlinearity and non-convexity of the MPC problem, the iterative MPC is not ensured to provide a performance cost converging to that corresponding to the centralized MPC.

REFERENCES

[1] S. M. Amin and B. F. Wollenberg, "Toward a smart grid," *IEEE Power Energy Mag.*, vol. 3, pp. 34–41, Apr. 2008.
[2] U.S. Department of Energy, Washington, DC, "The Smart Grid: An Introduction," Tech. Rep., 2008.
[3] California Energy Commission, Sacramento, CA, "Integrating new and emerging technologies into the California smart grid infrastructure," Tech. Rep., 2008.
[4] P. Novak, T. Ekelund, Y. Jovik, and B. Schmidtbauer, "Modeling and control of variable-speed wind-turbine drive system dynamics," *IEEE Control Syst. Mag.*, vol. 15, no. 4, pp. 28–37, Aug. 1995.
[5] F. Valenciaga, P. F. Puleston, and P. E. Battaiotto, "Variable structure system control design method based on a differential geometric approach: Application to a wind energy conversion subsystem," *IEE Proc.—Control Theory Appl.*, vol. 151, pp. 6–12, 2004.

[6] M. Chinchilla, S. Arnaltes, and J. C. Burgos, "Control of permanent-magnet generators applied to variable-speed wind-energy systems connected to the grid," *IEEE Trans. Energy Conv.*, vol. 21, no. 1, pp. 130–135, Mar. 2006.

[7] M. S. Khan and M. R. Iravani, "Hybrid control of a grid-interactive wind energy conversion system," *IEEE Trans. Energy Conv.*, vol. 23, no. 3, pp. 895–902, Sep. 2008.

[8] T. A. Johansen and C. Storaa, "Energy-based control of a distributed solar collector field," *Automatica*, vol. 38, pp. 1191–1199, 2002.

[9] E. F. Camacho and M. Berenguel, "Robust adaptive model predictive control of a solar plant with bounded uncertainties," *Int. J. Adapt. Control Signal Process.*, vol. 11, pp. 311–325, 1997.

[10] N. Hamrouni, M. Jraidi, and A. Cherif, "New control strategy for 2-stage grid-connected photovoltaic power system," *Renewable Energy*, vol. 33, pp. 2212–2221, 2008.

[11] F. Valenciaga, P. F. Puleston, P. E. Battaiotto, and R. J. Mantz, "Passivity/sliding mode control of a stand-alone hybrid generation system," *IEE Proc.—Control Theory Appl.*, vol. 147, pp. 680–686, 2000.

[12] F. Valenciaga, P. F. Puleston, and P. E. Battaiotto, "Power control of a photovoltaic array in a hybrid electric generation system using sliding mode techniques," *IEE Proc.—Control Theory Appl.*, vol. 148, pp. 448–455, 2001.

[13] F. Valenciaga and P. F. Puleston, "Supervisor control for a stand-alone hybrid generation system using wind and photovoltaic energy," *IEEE Trans. Energy Conv.*, vol. 20, no. 2, pp. 398–405, Jun. 2005.

[14] N. A. Ahmed, M. Miyatake, and A. K. Al-Othman, "Hybrid solar photovoltaic/wind turbine energy generation system with voltage-based maximum power point tracking," *Electric Power Compon. Syst.*, vol. 37, pp. 43–60, 2009.

[15] M. Dali, J. Belhadj, and X. Roboam, "Hybrid solar-wind system with battery storage operating in grid-connected and standalone mode: Control and energy management—Experimental investigation," *Energy*, vol. 35, pp. 2587–2595, 2010.

[16] W. Qi, J. Liu, X. Chen, and P. D. Christofides, "Supervisory predictive control of stand-alone wind-solar energy generation systems," *IEEE Trans. Control Syst. Technol.*, vol. 19, no. 1, pp. 199–207, Jan. 2011.

[17] W. Qi, J. Liu, and P. D. Christofides, "Supervisory predictive control for long-term scheduling of an integrated wind/solar energy generation and water desalination system," *IEEE Trans. Control Syst. Technol.*, 10.1109/TCST.2011.2119318.

[18] W. Qi, J. Liu, and P. D. Christofides, "A distributed control framework for smart grid development: Energy/water system optimal operation and electric grid integration," *J. Process Control*, vol. 21, pp. 1504–1516, 2011.

[19] E. Camponogara, D. Jia, B. H. Krogh, and S. Talukdar, "Distributed model predictive control," *IEEE Control Syst. Mag.*, vol. 22, no. 1, pp. 44–52, Feb. 2002.

[20] R. Scattolini, "Architectures for distributed and hierarchical model predictive control—A review," *J. Process Control*, vol. 19, pp. 723–731, 2009.

[21] A. N. Venkat, I. A. Hiskens, J. B. Rawlings, and S. J. Wright, "Distributed MPC strategies with application to power system automatic generation control," *IEEE Trans. Control Syst. Technol.*, vol. 16, no. 6, pp. 1192–1206, Nov. 2008.

[22] B. T. Stewart, A. N. Venkat, J. B. Rawlings, S. J. Wright, and G. Pannocchia, "Cooperative distributed model predictive control," *Syst. Control Lett.*, vol. 59, pp. 460–469, 2010.

[23] J. Liu, X. Chen, D. M. de la Peña, and P. D. Christofides, "Sequential and iterative architectures for distributed model predictive control of nonlinear process systems," *AIChE J.*, vol. 56, pp. 2137–2149, 2010.

[24] E. Camponogara and H. F. Scherer, "Distributed optimization for model predicitve control of linear dynamic networks with control-input and output constraints," *IEEE Trans. Autom. Sci. Eng.*, vol. 8, no. 1, pp. 233–242, Jan. 2011.

[25] A. Costa, A. Crespo, J. Navarro, G. Lizcano, H. Madsen, and E. Feitosa, "A review on the young history of the wind power short-term prediction," *Renewable Sustainable Energy Rev.*, vol. 12, pp. 1725–1744, 2008.

[26] , D. Linden and T. B. Reddy, Eds*., Handbook of Batteries*, 3rd ed. New York: McGraw-Hill, 2002.

[27] A. J. Ruddell, A. G. Dutton, H. Wenzl, C. Ropeter, D. U. Sauer, J. Merten, C. Orfanogiannis, J. W. Twidell, and P. Vezin, "Analysis of battery current microcycles in autonomous renewable energy systems," *J. Power Sources*, vol. 112, pp. 531–546, 2002.

[28] A. Wächter and L. T. Biegler, "On the implementation of primal-dual interior point filter line search algorithm for large-scale nonlinear programming," *Math. Program.*, vol. 106, pp. 25–57, 2006.